Stochastic Processes in Multi-occupancy Lattice Systems

A thesis submitted in partial fulfillment of the requirements
for the degree of Bachelor of Science and Master of Science

by

Swastik Majumder
Roll Number: 20MS175

DEPARTMENT OF PHYSICAL SCIENCES
INDIAN INSTITUTE OF SCIENCE EDUCATION AND RESEARCH
KOLKATA

Supervisor: Professor Mustansir Barma
Tata Institute of Fundamental Research, Hyderabad

Coordinator: Dr. Anandamohan Ghosh
Indian Institute of Science Education and Research Kolkata

May, 2025

Declaration by the student

Date: 3^{rd} May, 2025.

I, Mr. Swastik Majumder Registration No. 20MS175 dated 3^{rd} May, 2025, a student of the Department of Physical Sciences of the BS-MS Programme of IISER Kolkata, hereby declare that this thesis is my own work and, to the best of my knowledge, it neither contains materials previously published or written by any other person, nor has it been submitted for any degree/diploma or any other academic award anywhere before. I have used the originality checking service to prevent inappropriate copying.

I also declare that all copyrighted material incorporated into this thesis is in compliance with the Indian Copyright Act, 1957 (amended in 2012) and that I have received written permission from the copyright owners for my use of their work.

I hereby grant permission to IISER Kolkata to store the thesis in a database which can be accessed by others.

Signature
Swastik Majumder
Department of Physical Sciences
Indian Institute of Science Education and Research Kolkata

Mohanpur 741246, West Bengal, India

Certificate from the Supervisor

Date: 3^{rd} May, 2025.

This is to certify that the thesis titled "Stochastic Processes in Multi-occupancy Lattice Systems" submitted by Mr. Swastik Majumder Registration No. 20MS175 dated 3^{rd} May 2025, a student of the Department of Physical Sciences of the BS MS Programme of IISER Kolkata, is based upon his own research work under my supervision. I also certify, to the best of my knowledge, that neither the thesis nor any part of it has been submitted for any degree/diploma or any other academic award anywhere before. In my opinion, the thesis fulfils the requirement for the award of the degree of Bachelor of Science and Master of Science.

Signature
Mustansir Barma
Professor Emeritus
Tata Institute of Fundamental Research, Hyderabad.

Acknowledgements

I would like to extend my heartfelt gratitude to everyone who has supported and guided me throughout my academic journey and during the completion of this thesis.

First and foremost, I sincerely thank my supervisor, Professor Mustansir Barma, for his unwavering guidance, invaluable support, and encouragement throughout my project. Every meeting with him was an enriching experience, offering deep insights and learning opportunities. His constructive suggestions and advice have been instrumental in shaping my thesis and enhancing my academic growth beyond this work. I am also deeply appreciative of TIFR, Hyderabad, for graciously hosting me during my visits there. The resources available at TIFR-H played a key role in advancing my research. I am also truly thankful to Dr. Anandamohan Ghosh, my thesis coordinator, for closely monitoring my progress throughout my work.

I am profoundly grateful to my parents for their constant support and unwavering belief in me throughout my academic journey at IISER Kolkata. Without them, I would not have come this far.

I would also like to express my heartfelt thanks to Manasvini Subramanian for her enduring support and patience during my time at IISER Kolkata. Her encouragement and understanding have been a great source of strength, and I am truly thankful for her presence through every challenge and triumph. I'm incredibly thankful to Arabdha Bhattacharya for our long-time friendship and for always being there during my stay in Kolkata since we were kids.

Lastly, I wish to express my sincere appreciation to my friends—Aakash Kumar, Rohan Didmishe, and Ankan Basak—for making my time at IISER Kolkata more engaging. Our discussions, spanning from physics to philosophy, and their companionship have been a central part of my life here, and I am genuinely grateful for their friendship.

Abstract

This thesis explores aspects of non-equilibrium statistical mechanics through the study of interacting particle systems on simple lattice structures, including rings, branched geometries, percolation-like backbones, and random combs. These systems lie between the zero-range process and the asymmetric simple exclusion process in terms of their dynamics and interaction rules. In the models considered, each site can accommodate an arbitrary number of particles, with local energy costs associated with occupation. Particle dynamics are governed by stochastic rules influenced by both interaction energies and external bias.

We analyze these systems using a combination of numerical simulations and analytical methods, focusing on steady-state properties under different boundary conditions. Key results include characterizations of stationary distributions, density profiles, steady state currents and two-point correlations. For systems with periodic boundary conditions, we identify an effective mapping in the regime of strong interactions, along with non-monotonic behavior in density correlations as a function of interaction strength.

These findings provide a quantitative understanding of how interaction strength, bias, system geometry, and boundary conditions affect the steady-state behavior of driven lattice systems.

Contents

List of Figures

Dedicated to Mum.

Chapter 1

Introduction

1.1 Motivation and Background

Statistical mechanics offers a foundational framework for linking the microscopic dynamics of individual constituents to the emergent macroscopic behavior of complex systems. Within this domain, equilibrium statistical mechanics [1] has achieved profound success in describing systems that reach time-independent statistical states governed by a set of macroscopic constraints. Its strength lies in both its universality and its predictive power: given the microscopic Hamiltonian and constraints such as temperature, volume, and particle number, one can derive the system's thermodynamic properties through well-defined principles.

A cornerstone of equilibrium statistical mechanics is the concept of the *ensemble*—a theoretical construct representing a large collection of identically prepared systems under common macroscopic conditions. For instance, in the canonical ensemble, systems are in thermal equilibrium with a heat bath at temperature T, and the thermodynamic behavior is encapsulated in the partition function $\mathcal{Z}$:

$$\mathcal{Z} = \sum_{i \in \{\text{states}\}} \exp\left(-\beta \mathcal{H}_i\right), \tag{1.1}$$

where $\beta = 1/k_B T$ is the inverse temperature, k_B is Boltzmann's constant, and $\mathcal{H}_i$ denotes the Hamiltonian of microstate i.

This formalism applies to a vast range of physical systems. In ideal gases, the microstates are specified by the positions and momenta of all particles. In magnetic systems like the Ising model, states correspond to spin configurations on a lattice. In polymeric systems, microstates represent conformations of polymer chains, and so on.In principle, the partition function provides a means to calculate key thermodynamic quantities such as free energy, internal energy, entropy, and specific heat, while also facilitating the analysis of fluctuations, among other aspects.

However, many systems of physical interest lie beyond the reach of equilibrium statistical mechanics. These include systems driven by external forces, connected to multiple reservoirs with differing thermodynamic parameters, or undergoing intrinsically time-dependent processes. Examples include conductors under voltage bias, driven diffusive systems such as the asymmetric exclusion process [2]. In such cases, the system is maintained in a nonequilibrium steady state (NESS), characterized by non-vanishing probability currents in configuration space and a breakdown of time-reversal symmetry.

Describing nonequilibrium systems introduces considerable challenges. There is no universal prescription for assigning probabilities to microstates under nonequilibrium conditions, and steady-state distributions generally cannot be derived from variational principles analogous to those in equilibrium. As a consequence, each system may be treated on a case-by-case basis. The absence of a general form for steady-state distributions or a variational principle implies that theoretical progress relies heavily on the detailed study of representative models, supported by both analytical and computational tools. Such studies are essential for identifying universal features of nonequilibrium behavior and for guiding the development of new theoretical frameworks.

1.2 Organization and Contents of the Thesis

This thesis is devoted to the study of driven lattice systems in which multiple particles can occupy each site, subject to soft, finite repulsive interactions. These systems represent an intermediate regime between non-interacting and hard-core interacting

systems, and are of particular interest under nonequilibrium conditions where sustained particle transport and nontrivial steady states emerge.

The dynamics of these models are governed by stochastic particle hopping between neighboring sites, influenced by both interaction strength and external bias. In contrast to systems with hard-core exclusion, where multiple occupancy is strictly forbidden, the models studied here allow for multiple occupancy. This includes interaction-induced modulations of particle currents and non-monotonic spatial correlations as a function of interaction strength.

The thesis is structured as follows:

- **Chapter 2** introduces the master equation formalism, which provides the analytical foundation for describing the time evolution of probability distributions in stochastic systems.
- **Chapter 3** and **Chapter 4** present two well-established nonequilibrium models—the Zero-Range Process (ZRP) and the Asymmetric Simple Exclusion Process (ASEP)—highlighting their steady-state properties and the phenomena of current generation and condensation. These models serve as benchmarks for comparison with the interacting systems considered later.
- **Chapter 5** focuses on systems of repulsively interacting particles driven in an external field through different geometries such as percolation backbones, random branches, and comb-like structures. These settings provide minimal models for disordered substrates and reveal how geometry and interactions jointly affect transport.
- **Chapter 6** investigates one-dimensional systems with periodic boundary conditions and reflecting boundary conditions. Here, the effects of repulsion and asymmetry in choice of hopping direction are explored both analytically and numerically. Results include particle currents, correlation functions, and limiting behaviors such as the linear response and strong interaction regimes. The results are strongly dependent on the boundary conditions.
- **Chapter 7** summarizes the main findings of the thesis, situates them within the broader landscape of nonequilibrium statistical mechanics, and outlines possible directions for future research.

This page is intentionally left blank.

Chapter 2

The Master Equation in Stochastic Processes

2.1 Introduction

Stochastic processes [3] provide a rigorous framework for modeling systems that evolve probabilistically over time. These processes are fundamental to various disciplines, including statistical physics, chemical kinetics, systems biology, and financial mathematics. The early development of stochastic theory can be traced back to Bachelier, who introduced the concept of a random walk to model fluctuations in financial markets. This concept was later instrumental in understanding Brownian motion, with foundational work by Einstein, Smoluchowski, and Langevin.

Unlike deterministic systems, where the future state is entirely determined by the current state and the system's dynamics, stochastic systems are influenced by random factors. As a result, their evolution is most effectively described using probability distributions over potential states.

A particularly significant class of stochastic processes is the *Markov process*, where the system's future behavior depends only on its present state and not on the sequence of states that preceded it. This property, known as the *Markov property*, was first formalized by A.A. Markov in 1906. The evolution of probability distributions

in such processes is described by the *master equation*, initially introduced by Pauli in the context of quantum transitions.

2.2 The Master Equation Formalism

Let $P(\mathcal{C}, t)$ denote the probability that the system is in configuration $\mathcal{C}$ at time t. The master equation, which governs the time evolution of this probability, is expressed as:

$$\frac{d}{dt}P(\mathcal{C}, t) = \sum_{\mathcal{C}'} \left[W(\mathcal{C}' \to \mathcal{C})P(\mathcal{C}', t) - W(\mathcal{C} \to \mathcal{C}')P(\mathcal{C}, t) \right], \tag{2.1}$$

where $W(\mathcal{C}' \to \mathcal{C})$ is the transition rate from state $\mathcal{C}'$ to $\mathcal{C}$. The first term on the right-hand side accounts for probability flux into $\mathcal{C}$, while the second term represents flux out of $\mathcal{C}$.

2.2.1 Matrix Representation of the Master Equation

The master equation can be reformulated in matrix notation for compactness and analytical convenience. Define the transition rate matrix $\mathbb{W}$, with elements given by:

$$\mathbb{W}_{mn} = W_{mn} - \delta_{mn} \sum_{k} W_{km}, \tag{2.2}$$

where m and n denote state indices, and δ_{mn} is the Kronecker delta. This form ensures that the diagonal elements reflect the total rate of exiting state n, while off-diagonal terms correspond to transitions between distinct states.

The master equation in vector form is:

$$\dot{P}(t) = \mathbb{W}P(t), \tag{2.3}$$

where $P(t)$ is the column vector of state probabilities. The formal solution to this equation is:

$$P(t) = e^{\mathbb{W}t}P(0), \tag{2.4}$$

which propagates the initial distribution $P(0)$ through the matrix exponential of $\mathbb{W}$.

Although solving this equation often involves diagonalizing $\mathbb{W}$, it is important to note that $\mathbb{W}$ is not necessarily symmetric and may not possess a complete set of orthonormal eigenvectors.

Two key properties characterize any valid transition rate matrix $\mathbb{W}$:

$$\mathbb{W}_{mn} \geq 0 \quad \text{for } m \neq n, \tag{2.5}$$

$$\sum_m \mathbb{W}_{mn} = 0, \quad \forall n. \tag{2.6}$$

A matrix satisfying these conditions is referred to as a $\mathbb{W}$-*matrix*. These properties guarantee the conservation of total probability and the non-negativity of transition rates.

2.3 Stationary States and Detailed Balance

For systems with a finite number of states, the long-time behavior is typically dominated by a stationary distribution $P^{SS}(\mathcal{C})$, defined by the condition:

$$\frac{d}{dt}P^{SS}(\mathcal{C}) = 0. \tag{2.7}$$

Substituting into the master equation yields:

$$\sum_{\mathcal{C}'} \left[W(\mathcal{C}' \to \mathcal{C})P^{SS}(\mathcal{C}') - W(\mathcal{C} \to \mathcal{C}')P^{SS}(\mathcal{C})\right] = 0. \tag{2.8}$$

A stronger condition than stationarity is the principle of *detailed balance*, which requires that for every pair of configurations:

$$W(\mathcal{C}' \to \mathcal{C})P^{SS}(\mathcal{C}') = W(\mathcal{C} \to \mathcal{C}')P^{SS}(\mathcal{C}). \tag{2.9}$$

This condition implies that the probability current between any two states vanishes in equilibrium, leading to a time-reversible dynamic at the statistical level. Systems in thermodynamic equilibrium, particularly those described by the Boltzmann distribution, typically satisfy this condition.

However, many systems of practical interest operate far from equilibrium and do not satisfy detailed balance. Examples include driven diffusive systems, active matter, and biological processes subject to external energy input. In such cases, the steady state may involve persistent probability currents and non-vanishing entropy production. In the later chapters, we shall mainly be focussing on steady state solutions to the master equation in consideration.

This page is intentionally left blank.

Chapter 3

Zero-Range Process (ZRP)

3.1 Introduction to the Zero Range Process

The Zero Range Process (ZRP) [4] is an interacting particle system extensively studied in statistical physics, probability theory, and its applications to non-equilibrium systems. In this process, particles hop between sites on a lattice, with the jump rate determined only by the number of particles at the departure site, independent of the occupancy of the target site. This feature distinguishes the ZRP from other interacting particle systems, such as the exclusion process.

3.1.1 Definition and Dynamics

Consider a lattice Λ, which may be finite or infinite (e.g., $\mathbb{Z}^d$). Each site $i \in \Lambda$ is occupied by an integer number of particles, denoted by $n_i \geq 0$. The system evolves as follows:

- A particle at site i attempts to jump to a neighboring site j at a rate $u(n_i)$, where $u(n)$ is a function of the occupancy n at site i.
- The destination site j is chosen according to a transition probability $p(i, j)$.

- The function $u(n)$ characterizes the interaction of the system and can lead to interesting phenomena, such as condensation, when $u(n)$ decays sufficiently slowly.

3.1.2 Master Equation

Let the state of the system at time t be represented by the vector $\mathbf{n}(t) = (n_i(t))_{i\in\Lambda}$. The time evolution of the probability distribution $P(\mathbf{n}, t)$ for the system configuration in the Zero Range Process (ZRP) is governed by the following master equation:

$$\frac{dP(\mathbf{n},t)}{dt} = \sum_{i,j}^{i\neq j} \left[u(n_i+1)p(i,j)P(\mathbf{n}^{i+1,j-1},t) - u(n_i)p(i,j)P(\mathbf{n},t)\right], \tag{3.1}$$

In this equation, $\mathbf{n}^{i+1,j-1}$ denotes the configuration obtained by transferring a particle from site i to site j.

3.1.3 Stationary Distribution

One of the most remarkable properties of the Zero Range Process is that, under appropriate conditions, its stationary distribution is given by a factorized form:

$$P(\mathbf{n}) = \frac{1}{\mathcal{Z}} \prod_{i\in\Lambda} f(n_i), \tag{3.2}$$

where $\mathcal{Z}$ is a normalization factor and $f(n)$ is determined by the jump rates $u(n)$. This property makes ZRP analytically tractable and useful for studying non-equilibrium steady states.

3.2 Solution of the Zero Range Process on a Ring

In a one dimensional lattice with periodic boundary conditions, we consider L sites, labeled $l = 1, 2, \ldots, L$, with occupancies n_i at a given site i, such that,

$$\sum_{i=1}^{L} n_i = N. \tag{3.3}$$

We further assume that particles can hop only clockwise (or only anticlockwise) at a transition rate $u(n_i)$. The probability of a configuration $\mathbf{n} = (n_1, n_2, \ldots, n_L)$ is given by 3.2, where the normalization is the canonical partition function and is given by,

$$\mathcal{Z}_{N,L} = \sum_{n_1,n_2,\ldots,n_L} \prod_{l=1}^{L} f(n_l)\delta\left(\sum_{i=1}^{L} n_i - N\right). \tag{3.4}$$

The factor $f(n_l)$ is given by,

$$f(n) = \prod_{i=1}^{n} u(i)^{-1} \quad \text{for } n > 0, \quad f(0) = 1. \tag{3.5}$$

Proof. In the steady state we have from 3.1,

$$0 = \sum_{i=1}^{L} [u(n_{i-1}+1)P(\ldots, n_{i-1}+1, n_i - 1, \ldots) - u(n_i)P(n_1, \ldots, n_L)] \tag{3.6}$$

We substitute the factorized form 3.5 into 3.6 to perform the cancellation, thus

$$u(n_{i-1}+1)\frac{f(n_{i-1}+1)}{f(n_{i-1})} = u(n_i)\frac{f(n_i)}{f(n_i - 1)} = \text{constant}. \tag{3.7}$$

This constant can be normalized to unity without affecting the generality.

$$f(n_l) = \frac{f(n_l - 1)}{u(n_l)}. \tag{3.8}$$

The above expression 3.8 can be iterated to obtain 3.5, and where $f(0)$ can be set to unity. □

3.2.1 General results

The single site weight, which is the probability that a given site contains n particles will be given by,

$$p(n) = f(n)\frac{\mathcal{Z}_{L-1,N-n}}{\mathcal{Z}_{L,N}} = \sum_{n_2,\ldots,n_L} P(n, n_2, \ldots, n_L)\delta\left(\sum_{l=2}^{L} n_l - (N-n)\right) \tag{3.9}$$

Similarly the current j is simply given by,

$$j = \langle u(n_i)\rangle = \frac{1}{\mathcal{Z}_{N,L}} \sum_{n_1=0}^{N} \cdots \sum_{n_L=0}^{N} u(n_i) \prod_{l=1}^{L} f(n_l)\delta\left(\sum_{i=1}^{L} n_i - N\right) \tag{3.10}$$

We now use (3.8) to cancel the rate term to obtain,

$$j = \frac{1}{\mathcal{Z}_{N,L}} \sum_{n_1=0}^{N} \cdots \sum_{n_L=0}^{N} f(n_1 - 1) \prod_{l=2}^{L} f(n_l)\delta\left(\sum_{i=1}^{L} n_i - N\right) = \frac{\mathcal{Z}_{N-1,L}}{\mathcal{Z}_{N,L}}. \tag{3.11}$$

Thus, the mean hop rate or the current in the asymmetric case is as expected independent of the lattice site. We also have a useful result of recursion between the partition functions,

$$\mathcal{Z}_{N,L} = \sum_{n_1=0}^{N} \cdots \sum_{n_L=0}^{N} \prod_{l=1}^{L} f(n_l)\delta\left(\sum_{i=1}^{L} n_i - N\right) = \sum_{n=0}^{N} f(n) \prod_{l=2}^{L} f(n_l)\delta\left(\sum_{i=1}^{L} n_i - (N-n)\right). \tag{3.12}$$

This gives us,

$$\mathcal{Z}_{N,L} = \sum_{n=0}^{N} f(n)\mathcal{Z}_{N-n,L-1}. \tag{3.13}$$

We make a passing remark which has been proved in [4], that the steady state factorizes in an arbitrary lattice too, where, the hop rates from site l to site k, $u_{kl}(n_l)$ has the general form

$$u_{kl}(n_l) = u_l(n_l)W_{kl}, \tag{3.14}$$

where $u_l(n_l)$ is a site and occupancy dependent function of the departure site. W_{kl} is the probability that the particles hops to the site k. By conservation of probability

we have,

$$\sum_k W_{kl} = 1, \quad \forall l. \tag{3.15}$$

Thus, we see that if the matrix W_{kl} is not symmetric then the hopping rates are biased, which introduces heterogeneity in hopping dynamics. The steady state measure again factorizes to give, where the weight at each site is given by,

$$f_l(n_l) = \prod_{l=1}^{n_l} \frac{s_l}{u_l(i)}, \quad f(0) = 1, \tag{3.16}$$

where s_l represent the steady-state weights of a non interacting particle performing random walks, with the transition rates W_{lk} that satisfy:

$$s_l = \sum_k s_k W_{lk}. \tag{3.17}$$

3.2.2 Results in the grand canonical ensemble

The grand canonical partition function $\mathcal{Z}_L(z)$ is defined as,

$$\mathcal{Z}_L(z) = \sum_{n=0}^{\infty} z^n \mathcal{Z}_{L,N}. \tag{3.18}$$

z denotes the fugacity which fixes the average density ρ through,

$$\rho = \frac{z}{L}\frac{\partial ln \mathcal{Z}_L}{\partial z} = z\frac{F^{'}(z)}{F(z)}. \tag{3.19}$$

Using 3.4 we can obtain,

$$\mathcal{Z}_L(z) = \sum_{n_1=0}^{\infty} \cdots \sum_{n_L=0}^{\infty} z^{\sum_i n_i} \prod_{l=1}^{L} f(n_l) = [F(z)]^L, \tag{3.20}$$

where $F(z)$ is given by,

$$F(z) = \sum_{m=0}^{\infty} z^m f(m). \tag{3.21}$$

Quantities like $p(n)$, j defined in 3.9 and 3.10 can now be obtained as,

$$p(n) = z^n \frac{f(n)}{F(n)}. \tag{3.22}$$

$$j = \langle u(n) \rangle = \sum_{n=0}^{\infty} u(n)p(n) = \frac{1}{F(z)} \sum_{n=0}^{\infty} z^n u(n) f(n) \tag{3.23}$$

$$j = z \frac{1}{F(z)} \sum_{n=1}^{\infty} z^{n-1} f(n-1) = z. \tag{3.24}$$

This gives a physical interpretation of the fugacity z. This should be compared with $\langle u \rangle$ in the canonical ensemble given by 3.11. In Chapter 5 we shall see that the dynamics of the backbone can be mapped to a ZRP like process, allowing a total analytic hold on the steady state properties.

3.2.3 Condensation in the Zero-Range Process

A fascinating phenomenon observed in the Zero-Range Process (ZRP) is condensation, where a significant portion of the total mass (or particles) accumulates at a single site as the system reaches the thermodynamic limit.

Condensation occurs when the hopping rate $u(n)$ decreases sufficiently rapidly with increasing n. Specifically, for a given particle density ρ, condensation is seen when the single-site partition function of the stationary distribution has a finite critical density ρ_c. If the total density ρ surpasses ρ_c, the excess particles accumulate at a single site, resulting in the formation of a macroscopic cluster.

Condensation in the ZRP has been extensively explored in statistical physics, with applications to phenomena such as granular clustering, wealth condensation in economic models, and network congestion. Investigating these processes sheds light on non-equilibrium phase transitions and large deviation theory. A comprehensive review on condensation in the ZRP can be found in [4].

This page is intentionally left blank.

Chapter 4

Simple Exclusion Process

4.1 Introduction and Historical Background

The Simple Exclusion Process (SEP) is a paradigm non equilibrium system that plays a crucial role in the study of interacting particle systems. It provides a minimal model [2] for understanding transport phenomena, collective dynamics, and fluctuation theory in various physical and biological systems. The Symmetric Exclusion Process (SEP) involves particles moving on a discrete lattice, governed by straightforward stochastic rules that enforce an exclusion principle: at any given time, each site can be occupied by no more than one particle.

In particular, the asymmetric simple exclusion process (ASEP), a variant of the SEP in which particles move preferentially in one direction, has received significant attention. The exact solvability of certain cases of SEP and ASEP has been demonstrated using techniques such as the matrix product ansatz as discussed in [5].

4.2 Solution of ASEP on a Ring

We examine the Asymmetric Simple Exclusion Process (ASEP) on a one-dimensional lattice with periodic boundary conditions. The system is composed of L sites, labeled

by $i = 1, 2, \ldots, L$, each of which can be either occupied ($n_i = 1$) or unoccupied ($n_i = 0$). The total number of particles is conserved and satisfies,

$$\sum_{i=1}^{L} n_i = N \leq L. \tag{4.1}$$

The particles undergo stochastic dynamics characterized by biased hopping. The transition rates for particle movement are given by

$$W\left((n_i, n_{i+1}) \to (n_i - 1, n_{i+1} + 1)\right) = \frac{1}{2}(1+g)n_i(1-n_{i+1}), \tag{4.2}$$

$$W\left((n_i, n_{i+1}) \to (n_i + 1, n_{i+1} - 1)\right) = \frac{1}{2}(1-g)n_{i+1}(1-n_i), \tag{4.3}$$

where $g \in [0, 1]$ quantifies the asymmetry (or bias) in the hopping dynamics.

In the long-time limit, the system settles into a steady state where all microstates with exactly N particles have the same probability, independent of the value of g. Therefore, the steady-state probability distribution can be written as:

$$P(n_1, \ldots, n_L) = \frac{1}{\binom{L}{N}} \delta\left(\sum_{i=1}^{L} n_i - N\right). \tag{4.4}$$

Owing to the translational invariance of the system, the average occupation number at each site is uniform and is defined as

$$\langle n_i \rangle = \rho = \frac{N}{L}, \tag{4.5}$$

where ρ is the particle density.

The canonical partition function for this system is given by

$$\mathcal{Z}_{N,L} = \sum_{n_1=0}^{1} \cdots \sum_{n_L=0}^{1} \frac{1}{\binom{L}{N}} \delta\left(\sum_{i=1}^{L} n_i - N\right). \tag{4.6}$$

We now compute the probability that a given site is unoccupied. Without loss of generality, consider site 1. This probability is given by

$$P(0) = \frac{1}{\mathcal{Z}_{N,L}} \sum_{n_2=0}^{1} \cdots \sum_{n_L=0}^{1} \frac{1}{\binom{L}{N}} \delta\left(\sum_{i=2}^{L} n_i - N\right). \tag{4.7}$$

Recognizing that choosing N particles from L sites such that site 1 is empty is equivalent to choosing N particles from the remaining $L-1$ sites, we obtain

$$P(0) = \frac{1}{\mathcal{Z}_{N,L}} \sum_{n_2=0}^{1} \cdots \sum_{n_L=0}^{1} \frac{L-N}{L} \frac{1}{\binom{L-1}{N}} \delta\left(\sum_{i=2}^{L} n_i - N\right)$$

$$P(0) = (1-\rho)\, \frac{\mathcal{Z}_{N,L-1}}{\mathcal{Z}_{N,L}}. \tag{4.8}$$

In the thermodynamic limit $L \to \infty$, the ratio of partition functions in 4.8 tends to unity, and the system becomes uncorrelated, approaching a product measure. Therefore, we have

$$P(0) = 1 - \rho, \quad P(1) = \rho. \tag{4.9}$$

To study spatial correlations in the steady state, we define the two-point correlation function $G(r)$ as

$$G(r) = \langle n_i n_{i+r} \rangle - \langle n_i \rangle \langle n_{i+r} \rangle. \tag{4.10}$$

For $r \neq 0$, the steady-state product measure implies factorization of averages, yielding

$$G(r) = 0, \quad \text{for } r \neq 0. \tag{4.11}$$

At $r = 0$, the correlation function measures the variance of the occupation number. For hard-core particles, the identity $n_i^k = n_i$ holds for all $k \in \mathbb{R}$, hence

$$\mathbb{E}(n_i^k) = \langle n_i^k \rangle = \rho. \tag{4.12}$$

Using this in Eq. (4.10), we find

$$G(0) = \langle n_i^2 \rangle - \rho^2 = \rho(1-\rho), \tag{4.13}$$

which quantifies the fluctuations in particle number at a single site.

Finally, the steady-state particle current j in the thermodynamic limit is calculated using the net rate of rightward minus leftward hops:

$$j = \left\langle \frac{1}{2}(1+g)n_i(1-n_{i+1}) - \frac{1}{2}(1-g)n_{i+1}(1-n_i) \right\rangle = g\rho(1-\rho). \tag{4.14}$$

This current is maximal at half-filling ($\rho = 0.5$) and exhibits a non-monotonic dependence on density, as illustrated in Fig. 4.1.

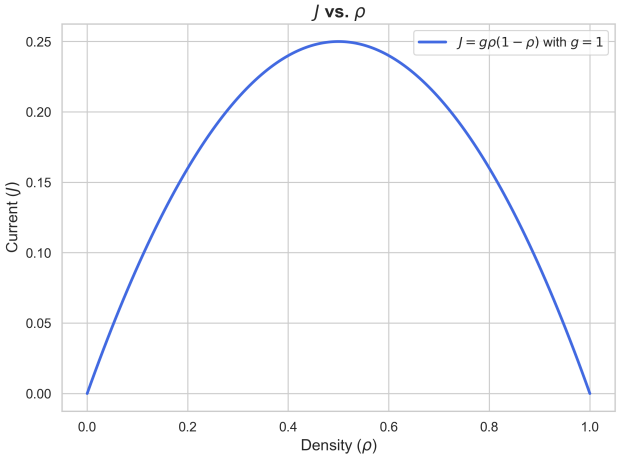

FIGURE 4.1: Steady-state current J as a function of density ρ, plotted for $g = 1$. The current follows the relation $J = g\rho(1-\rho)$, peaking at $\rho = 0.5$.

In the latter chapter, particularly in Chapter 6, we shall show how even with multiple occupancies unlike the ASEP, our model in certain limits is equivalent to an ASEP like process.

This page is intentionally left blank.

Chapter 5

Pairwise Interacting Particles in an External Field

5.1 Introduction

Previous studies, such as in [6] and [7], have explored the transport properties of non-interacting particles and hardcore particles respectively. These investigations have been carried out across various lattice geometries, including branches, backbones in percolation networks, and random combs, the latter serving as an approximation for random networks. In these systems, particle motion is influenced by both an external biasing field and by interactions or constraints between the particles, as detailed in the referenced works.

As discussed in [6], for non-interacting particles, a critical cutoff in the biasing parameter g exists, beyond which particles become trapped in the branches of a random comb. In this scenario, the effective drift velocity across the entire random comb exhibits a non-monotonic dependence on g and ultimately vanishes beyond the critical value of g. For hardcore particles [7], the drift velocity in the random comb remains non-monotonic with respect to g, but no trapping phenomenon is observed, except when the biasing field becomes infinite.

In this chapter, we explore an intermediate regime between non-interacting and hardcore particle cases. Specifically, we consider a system in which each lattice site

can accommodate an arbitrary number of particles, with an energy penalty incurred for multiple occupancies. The form of this on-site interaction energy is analogous to the Bose-Hubbard model [8], where particles experience pairwise repulsion.

The on-site repulsion is modeled by the pair wise energy function:

$$E(n_i) = \frac{U}{2} n_i(n_i - 1), \quad U \geq 0, \tag{5.1}$$

where U represents the strength of the repulsive interaction. This functional form suppresses high occupancies and significantly influences the system's dynamics by altering the transition rates.

In addition, the system is driven by an external biasing field. Under these conditions, we will demonstrate that under periodic boundary conditions, like the backbone of a percolation network, the model maps to a zero-range process (ZRP), for which exact steady-state solutions are known.

We examine this model across three distinct lattice geometries: (i) a one-dimensional lattice with periodic boundary conditions, analogous to the backbone structure of a percolation network; (ii) a one-dimensional lattice coupled to a reservoir at one end via a fugacity parameter, representing a branch; and (iii) a random comb lattice, which integrates both backbone and branch features, serving as an effective model for a percolation network.

5.2 Steady-State Results in a Backbone

Consider a configuration $\mathcal{C} = (n_1, \ldots, n_i, n_{i+1}, \ldots, n_L)$, where the system transitions to a new configuration $\mathcal{C}' = (n_1, \ldots, n_i - 1, n_{i+1} + 1, \ldots, n_L)$ due to a particle hopping from site i to site $i + 1$. In this analysis, periodic boundary conditions are assumed. The hopping rates are determined by enforcing the principle of local detailed balance.

By the principle of local detailed balance, the ratio of forward and backward hopping rates between configurations $\mathcal{C}$ and $\mathcal{C}'$ must satisfy the following relation:

$$\frac{W\left((n_i, n_{i+1}) \to (n_i - 1, n_{i+1} + 1)\right)}{W\left((n_i - 1, n_{i+1} + 1) \to (n_i, n_{i+1})\right)} = e^{-\beta(E(\mathcal{C}') - E(\mathcal{C}))}, \tag{5.2}$$

where β is the inverse temperature. The energy difference $\Delta E = E(\mathcal{C}') - E(\mathcal{C})$ arises from changes in the on-site interaction energies at sites i and $i+1$, in addition to the influence of the external uniform biasing field with strength Ea.

Using the definition in Eq. (5.1), we compute the energies for the bond between sites i and $i+1$ in the configurations $\mathcal{C}$ and $\mathcal{C}'$:

$$E(\mathcal{C}) = \frac{U}{2}\left[n_i(n_i-1) + n_{i+1}(n_{i+1}-1)\right] - Eakn_i - Ea(k+1)n_{i+1}, \tag{5.3}$$

$$E(\mathcal{C}') = \frac{U}{2}\left[(n_i-1)(n_i-2) + (n_{i+1}+1)(n_{i+1})\right] - Eak(n_i-1) - Ea(k+1)(n_{i+1}+1). \tag{5.4}$$

By subtracting the two expressions, we obtain the energy difference:

$$\Delta E = U(n_{i+1} - n_i + 1) - Ea. \tag{5.5}$$

Thus, the energy change associated with the hop depends linearly on the particle numbers at both the departure and arrival sites. A choice of hopping rates that satisfies the detailed balance condition in Eq. (5.2) is:

$$W\left((n_i, n_{i+1}) \to (n_i - 1, n_{i+1} + 1)\right) = \exp\left(\frac{\beta Ea}{2}\right) \exp\left(\beta U(n_i - 1)\right) \mathcal{I}_{n_i}, \tag{5.6}$$

$$W\left((n_i - 1, n_{i+1} + 1) \to (n_i, n_{i+1})\right) = \exp\left(-\frac{\beta Ea}{2}\right) \exp\left(\beta U(n_{i+1})\right), \tag{5.7}$$

where $\mathcal{I}_n$ is an indicator function, which is 0 if $n = 0$ and 1 otherwise. This setup provides a direct mapping to the zero-range process (ZRP) discussed in Chapter 3. In the grand canonical ensemble, the probability of a given configuration follows a product measure, given by:

$$P(\mathcal{C}) = \prod_{i=1}^{L} z^{n_i} f(n_i), \tag{5.8}$$

where $f(m)$ is defined as:

$$f(m) = \prod_{i=1}^{m} \frac{1}{e^{\beta U(n-1)}} = \exp\left(-\frac{\beta U}{2} m(m-1)\right), \quad f(0) = 1. \tag{5.9}$$

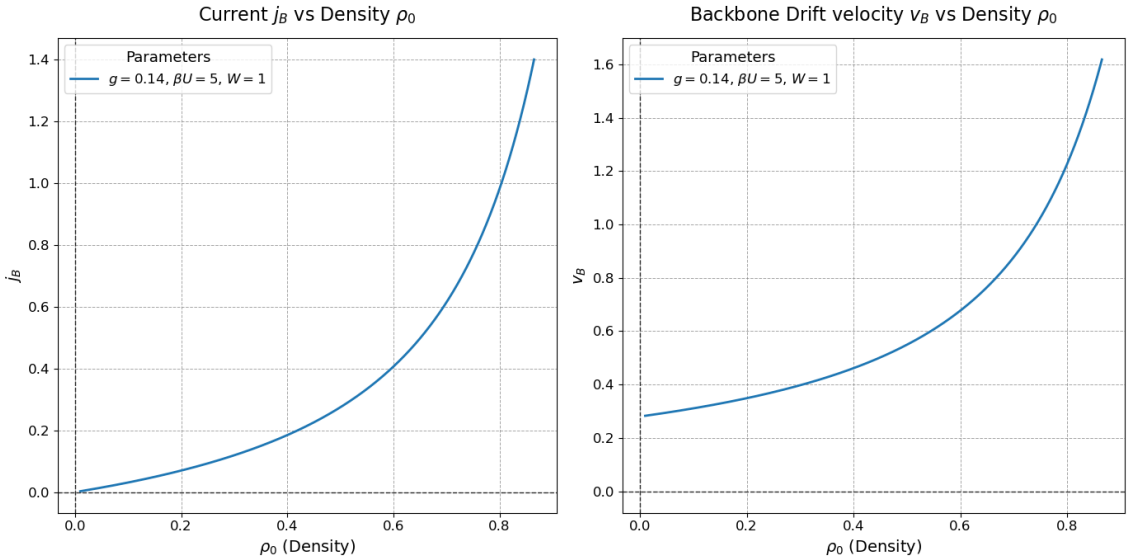

FIGURE 5.1: Plot of j_B vs ρ_0 with $\beta U = 5$ and plot of v_B with $\beta U = 5$.

The steady-state current j_B is then given by:

$$j_B = \left(e^{\frac{\beta E a}{2}} - e^{-\frac{\beta E a}{2}}\right) z, \tag{5.10}$$

where z is the fugacity. The fugacity is related to the backbone density ρ_0 through the following expression:

$$\rho_0 = z\frac{F'(z)}{F(z)}, \tag{5.11}$$

where $F(z)$ is defined as:

$$F(z) = \sum_{m=0}^{\infty} z^m f(m). \tag{5.12}$$

The density ρ_0 in the grand canonical ensemble can then be written as:

$$\rho_0 = \frac{\sum_{j=0}^{\infty} j z^j \exp\left(-\beta U \frac{j(j-1)}{2}\right)}{\sum_{j=0}^{\infty} z^j \exp\left(-\beta U \frac{j(j-1)}{2}\right)}. \tag{5.13}$$

Using the relations in Eqs. (5.10), (5.11), and (5.12), we can now obtain j_B as a function of ρ_0, and similarly, the drift velocity v_B as a function of ρ_0. The drift velocity v_B is the velocity of particles in the backbone, as illustrated in Figure 5.1. Both j_B and v_B are monotonically increasing functions of the backbone density ρ_0.

Finally, the term $e^{\beta Ea}$ is re-parameterized in terms of W and g as follows:

$$\frac{W(1+g)}{W(1-g)} = e^{\beta Ea}. \tag{5.14}$$

5.3 Steady state results in a branch

In the steady state, there is no current in the branch of length l, and the particles within this branch are characterized by the Hamiltonian,

$$\mathcal{H}(n_1, n_2, \ldots, n_L) = \sum_{k=0}^{l} \left(-Eakn_k + U\frac{n_k(n_k-1)}{2} \right) \tag{5.15}$$

The first term biases the particles to the right, whereas the second term introduces repulsive pair wise interactions between particles at the same site. The single site grand canonical partition function is then:

$$\mathcal{Z}(z,\beta) = \sum_{j=0}^{\infty} z^j exp\left(\beta Eakj - \beta U\frac{j(j-1)}{2} \right) \tag{5.16}$$

Introducing a fugacity z in the branch, one can obtain the density at each site in the branch using the grand canonical ensemble picture,

$$\rho_k = \frac{\sum_{j=0}^{\infty} jz^j exp\left(\beta Eakj - \beta U\frac{j(j-1)}{2}\right)}{\sum_{j=0}^{\infty} z^j exp\left(\beta Eakj - \beta U\frac{j(j-1)}{2}\right)} \tag{5.17}$$

This expression gives the average density at each site k in terms of fugacity z, biasing field E, position ak, and interaction term U. Due to the bias, each term is site-dependent, tending to increase the particle density toward higher-index sites. To approximate 5.17 , we apply the Euler-Maclaurin formula as detailed in [9]. We can approximate 5.16 as,

$$\mathcal{Z}(z,\beta) \approx \int_0^{\infty} z^x exp\left(\beta Eakx - \beta U\frac{x(x-1)}{2} \right) dx + \frac{1}{2}. \tag{5.18}$$

Redefining the variables,

$$A = \frac{\beta U}{2}, \quad B_k = lnz + \beta Eak + \frac{\beta U}{2}. \tag{5.19}$$

Then 5.18 can be written as,

$$\mathcal{Z}(z,\beta) = \int_0^\infty \exp\left(-Ax^2 + B_k x\right) dx + \frac{1}{2} = \frac{\sqrt{\pi}\, \mathrm{e}^{\frac{B_k^2}{4A}} \left(\mathrm{erf}\left(\frac{B_k}{2\sqrt{A}}\right) + 1\right)}{2\sqrt{A}} + \frac{1}{2}. \tag{5.20}$$

This ultimately can be written as,

$$\mathcal{Z}(z,\beta) = \frac{\sqrt{\pi}\, \exp\left(\frac{\left(\ln z + \beta Eak + \frac{\beta U}{2}\right)^2}{2\beta U}\right)}{\sqrt{2\beta U}} \left(\mathrm{erf}\left(\frac{\ln z + \beta Eak + \frac{\beta U}{2}}{\sqrt{2\beta U}}\right) + 1\right) + \frac{1}{2} \tag{5.21}$$

Similarly, we have,

$$\rho_k \approx \frac{1}{\mathcal{Z}(z,\beta)} \left(\frac{\partial}{\partial B_k} \left(\int_1^\infty z^x exp\left(\beta Eakx - \beta U \frac{x(x-1)}{2}\right)\right) + \frac{z}{2} \exp(\beta Eak)\right) \tag{5.22}$$

We compute the the first term of the numerator of 5.22,

$$\frac{\partial}{\partial B_k} \left(\int_1^\infty z^x exp\left(\beta Eakx - \beta U \frac{x(x-1)}{2}\right)\right) = \frac{\partial}{\partial B_k} \left(\frac{\sqrt{\pi}\, \mathrm{e}^{\frac{B_k^2}{4A}} \left(\mathrm{erf}\left(\frac{B_k - 2A}{2\sqrt{A}}\right) + 1\right)}{2\sqrt{A}}\right)$$

$$= \frac{\sqrt{\pi}\, B_k \mathrm{e}^{\frac{B_k^2}{4A}} \left(\mathrm{erf}\left(\frac{B_k - 2A}{2\sqrt{A}}\right) + 1\right)}{4A^{\frac{3}{2}}} + \frac{\mathrm{e}^{\frac{B_k^2}{4A} - \frac{(B_k - 2A)^2}{4A}}}{2A}$$

Thus we have,

$$\rho_k \approx \frac{1}{\mathcal{Z}(z,\beta)} \left[\frac{\sqrt{\pi}\left(\ln z + \beta Eak + \frac{\beta U}{2}\right) \exp\left(\frac{\left(\ln z + \beta Eak + \frac{\beta U}{2}\right)^2}{2\beta U}\right) \left(\mathrm{erf}\left(\frac{\ln z + \beta Eak - \frac{\beta U}{2}}{\sqrt{2\beta U}}\right) + 1\right)}{4\left(\frac{\beta U}{2}\right)^{3/2}} \right.$$

$$\left. + \frac{\exp\left(\frac{2\left(\ln z + \beta Eak + \frac{\beta U}{2}\right) - \beta U}{2\beta U}\right)}{\beta U} + \frac{z}{2} \exp(\beta Eak)\right]$$

We can add more correction terms through the B_l's as discussed in [9]. The behavior of ρ_k with different parameters are shown below,

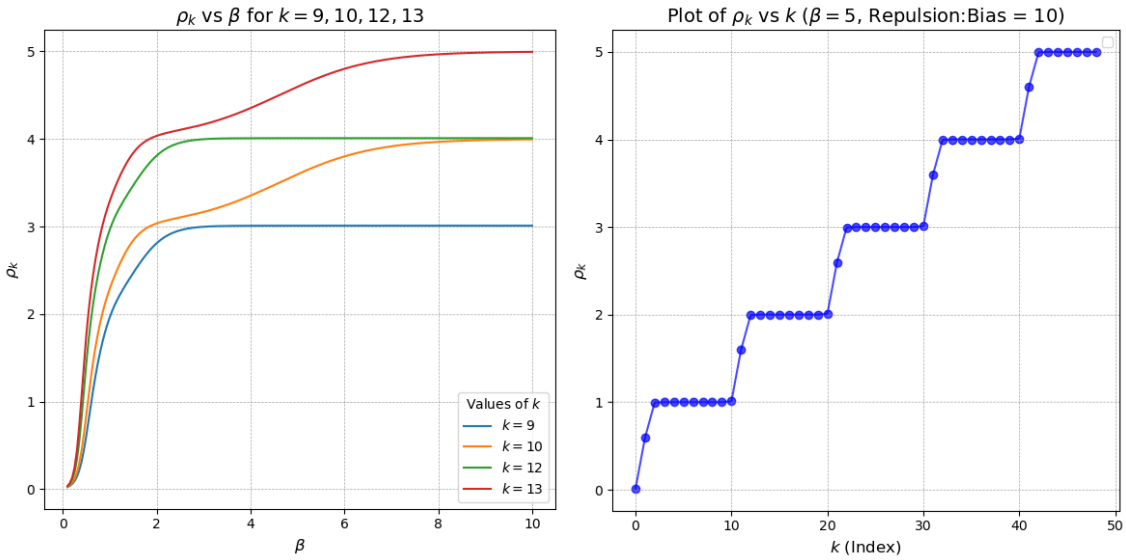

FIGURE 5.2: ρ_k vs β, with the ratio of repulsion versus biasing term as, $\frac{U}{Ea} = 3$ and ρ_k vs k, where k is the lattice index of the branch for $\beta = 5$ with the ratio of repulsion versus biasing term as, $\frac{U}{Ea} = 3$

- For the left plot in 5.2
  - The ρ_k vs β plot reveals a periodic modulation effect governed by the repulsion:bias ratio. This modulation determines the saturation values of ρ_k, with $k = 9$ saturating at 3, $k = 10$ at 4, and so on. The periodicity reflects the interplay between the energy contribution of k and the imposed bias, creating distinct plateaus that align with the modulation period.
- For the right plot in 5.2
  - For $U < Ea$, there is a monotonic linear increase in the average density as one moves deeper into the branch. For $U > Ea$ (as shown), the density shows a distinct stepwise growth, as illustrated above. Each step has unique features that we discuss further.
  - The average density at each site is an integer at very low temperatures.
  - For low temperatures, If $\frac{U}{Ea}$ is an integer greater than 1, then the length of each step corresponds to that ratio , as shown through energy minimization.

– For low temperatures, If $\frac{U}{Ea}$ is greater than 1 but not an integer, the step length can be found approximated by rounding the ratio,as seen by energy minimization.

5.4 Random Comb

A random comb [6] serves a toy model of a percolation network. It consists of a backbone, with branches of arbitrary lengths attached to each site in the backbone. We assign a distribution function of having a branch of length l of lattice spacing a, and percolation correlation length ζ,

$$P(l) = (1 - e^{-a/\zeta})e^{-al/\zeta} \tag{5.23}$$

A typical random comb can be visualized as follows, In the limit of a large backbone,

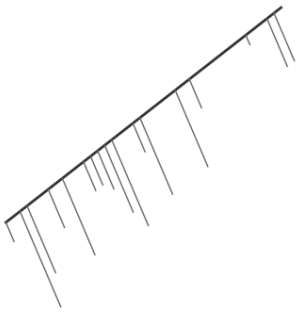

FIGURE 5.3: Random comb structure with a tilted backbone and branches.

that is the number of sites in the backbone going to ∞, it has been shown in [7] that the *macroscopic* drift velocity v_d in the overall comb is given by,

$$v_d = \frac{j_B}{\bar{n}}, \tag{5.24}$$

where, j_B is the backbone current, $\bar{n}$ is the average number of particles in a branch.

5.4.1 Comment on the growth of ρ_k

The growth of ρ_k with the depth of the branch is slower than linear growth, and as a result, the trapping behavior of particles as seen in [6] is mitigated for any finite strength of bias as the average number of particles in a branch in the random comb is finite, this can shown as follows, we have,

$$\rho_k \leq \alpha k + \rho_0, \quad \forall k. \tag{5.25}$$

where α is a function of $g, \beta U$. This can be easily shown from the energy minimization at $\beta \to \infty$. Then assuming a Poisson like distribution 5.23 of branch lengths in the percolation network, we have,

$$\bar{n} = \sum_{l=0}^{\infty} \mathcal{N} \exp\left(-al/\zeta\right) \sum_{k=0}^{l} \rho_k \leq \sum_{l=0}^{\infty} \mathcal{N} \exp\left(-al/\zeta\right) \left(\alpha \frac{l(l-1)}{2} + \rho_0 l\right) \tag{5.26}$$

$$= \frac{\alpha}{2}\mathbb{E}(l^2) + \left(\rho_0 - \frac{\alpha}{2}\right)\mathbb{E}(l).$$

Thus we have,

$$\bar{n} \leq \frac{\alpha}{2}\mathbb{E}(l^2) + \left(\rho_0 - \frac{\alpha}{2}\right)\mathbb{E}(l) < \infty. \tag{5.27}$$

5.4.2 Drift Velocity

The drift velocity v_d exhibits a non-monotonic dependence on the asymmetry parameter g. This behavior arises because the underlying density profiles $\bar{n}$ are not simple functions of g alone but also depend crucially on the product βU.

As g increases, one might naively expect the drift velocity to grow monotonically due to enhanced asymmetry; however, the situation is more intricate. The density $\bar{n}$ itself behaves non-monotonically with respect to g, because of competition between βU and g as, g is varied.

Moreover, for a fixed density ρ and a fixed asymmetry g, the drift velocity v_d saturates beyond a particular value of βU. Physically, this occurs because as U increases, the potential barriers between sites become increasingly dominant, and particles tend to localize more strongly within favorable regions, such as minima or branches in the

landscape. Consequently, beyond a certain threshold in βU, the branches become almost completely filled up to a characteristic density, and further increases in U no longer significantly affect the occupation probabilities. Since the drift velocity is ultimately governed by how easily particles can move across the potential landscape, once the branches are effectively filled, v_d reaches a plateau.

Thus, the overall behavior of v_d as a function of g and U results from a competition between asymmetry-driven transport and potential-dominated localization effects. The interplay between these two factors — controlled respectively by g and βU — underlies the non-monotonic structure observed in the drift velocity.

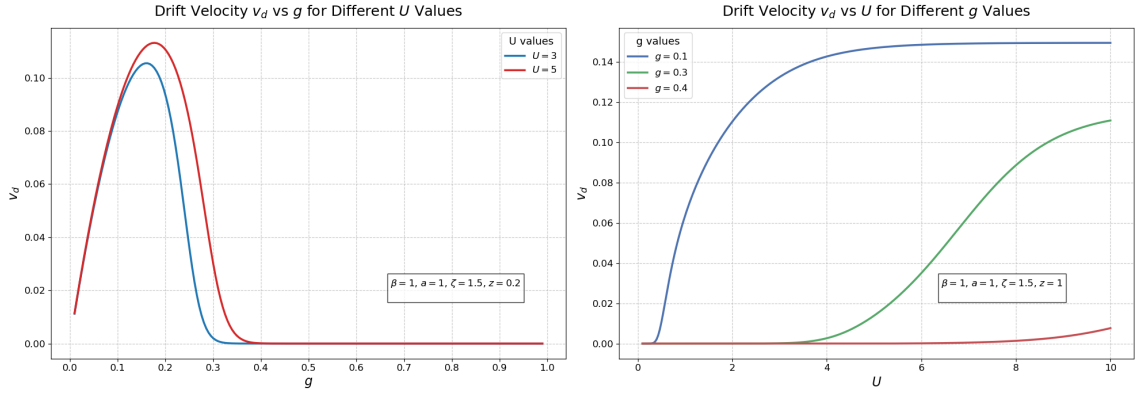

FIGURE 5.4: Comparison of the behavior of the drift velocity v_d with respect to (a) the asymmetry parameter g and (b) the interaction strength βU.

This page is intentionally left blank.

Chapter 6

Asymmetric Hopping in a Pairwise Interaction Model

6.1 Introduction and Motivation

In the previous chapter, we examined the effects of an external biasing field and on-site repulsion at a given site, which could be effectively mapped to a zero-range process (ZRP)–like stochastic model. In this chapter, we focus on the combined influence of on-site repulsion and stochastic directionality in such a way that the external field does not overshadow the interaction terms in the limit $g \to 1$.

Previously, the limit $g \to 1$ implied that the external field $F \to \infty$, rendering the influence of finite interaction strengths negligible. However, a more physically realistic scenario arises when $g \to 1$ simply leads to a totally asymmetric hopping in one direction, while the dynamics continue to be governed by on-site repulsion. This perspective allows for the incorporation of stochastic behavior driven by particle interactions rather than being dominated by an external field.

Furthermore, by choosing hopping rates that obey detailed balance with respect to internal energy considerations, we allow the hopping rates to depend on both the departure and arrival sites. This approach results in modeling of mass transport processes with on-site repulsion, where the dynamics reflect the effects of internal energies.

The model we study here is not only physically motivated and conceptually simple, but also exhibits a range of intriguing behaviors. These include interesting limiting behavior, non-monotonic correlations, and periodic oscillations in the steady-state current versus density in the large βU limit.

6.2 Setting up the Hopping Rates

Consider a configuration $\mathcal{C} = (n_1, \ldots, n_i, n_{i+1}, \ldots, n_L)$, which transitions to a new configuration $\mathcal{C}' = (n_1, \ldots, n_i - 1, n_{i+1} + 1, \ldots, n_L)$ due to a particle hopping from site i to site $i + 1$. As discussed in the previous chapter, each site can host an arbitrary number of particles, constrained only by the total number of particles N in the canonical ensemble.

6.2.1 Hopping Rates from Detailed Balance (Unbiased Case)

Assume first that there is no directional bias in the system. Then, by the principle of LDB, the ratio of forward and backward hopping rates between configurations $\mathcal{C}$ and $\mathcal{C}'$ must satisfy:

$$\frac{W\left((n_i, n_{i+1}) \to (n_i - 1, n_{i+1} + 1)\right)}{W\left((n_i - 1, n_{i+1} + 1) \to (n_i, n_{i+1})\right)} = e^{-\beta(E(\mathcal{C}') - E(\mathcal{C}))}, \tag{6.1}$$

where β is the inverse temperature. The energy difference $\Delta E = E(\mathcal{C}') - E(\mathcal{C})$ comes entirely from the change in on-site interaction energies at sites i and $i+1$. A choice of hopping rates that satisfies the detailed balance condition Eq. (6.1) is:

$$W\left((n_i, n_{i+1}) \to (n_i - 1, n_{i+1} + 1)\right) = \exp\left(-\frac{\beta U}{2}(n_{i+1} - n_i + 1)\right), \tag{6.2}$$

$$W\left((n_i - 1, n_{i+1} + 1) \to (n_i, n_{i+1})\right) = \exp\left(-\frac{\beta U}{2}(n_i - n_{i+1} - 1)\right). \tag{6.3}$$

We can now define the general form of the hopping rate from a site with m particles to a neighboring site with n particles as:

$$W(m,n) = \exp\left(-\frac{\beta U}{2}(n-m+1)\right)(1-\delta_{0,m}), \tag{6.4}$$

where the Kronecker delta ensures that hopping is only allowed if the departure site is not empty.

6.2.2 Introducing Bias in the Hopping Rates

To incorporate directional bias, we introduce a parameter $g \in [-1,1]$ that biases hopping preferentially in one direction without introducing singularities in the rate functions. The hopping rate from site i to $i+1$ (clockwise) is defined as:

$$W_c(n_i, n_{i+1}) = \frac{1+g}{2}\exp\left(-\frac{\beta U}{2}(n_{i+1}-n_i+1)\right)(1-\delta_{0,n_i}), \tag{6.5}$$

and the rate from site $i+1$ to i (anti-clockwise) is:

$$W_a(n_i, n_{i+1}) = \frac{1-g}{2}\exp\left(-\frac{\beta U}{2}(n_i-n_{i+1}+1)\right)\left(1-\delta_{0,n_{i+1}}\right). \tag{6.6}$$

In this formulation, the bias term $\frac{1\pm g}{2}$ controls the preference of directionality in hopping: for $g=0$, the dynamics are unbiased; for $g \to 1$, hopping becomes fully biased clockwise; and for $g \to -1$, it becomes fully biased anti-clockwise.

Thus, the direction of hopping is chosen probabilistically according to the bias parameter, and the rate of hopping is dominated by the local energy landscape arising from on-site interactions. This separation of bias and interaction ensures that, even in the strongly biased limit $g \to 1$, the dynamics remain finite and governed by interaction-driven processes rather than being dominated by the external bias.

6.3 Setting up the master equation

We now formulate the master equation that governs the time evolution of the probability distribution for configurations on a one-dimensional periodic lattice of length L, with periodic boundary conditions, i.e., $n_{i+L} = n_i$. A configuration of the system is denoted by $(n_1, \ldots, n_L)$, where n_i represents the number of particles at site i.

The system evolves stochastically via particle hopping, governed by the clockwise and anti-clockwise hopping rates W_c and W_a defined in Eqs. (6.5) and (6.6), respectively. The master align for the probability $P(n_1, \ldots, n_L; t)$ is given by

$$\begin{aligned}\frac{d}{dt}P(n_1,\ldots,n_L;t) = \sum_{i=1}^{L} \big[&W_c(n_{i-1}+1, n_i-1)\, P(\ldots, n_{i-1}+1, n_i-1, \ldots) \\ &+ W_a(n_i-1, n_{i+1}+1)\, P(\ldots, n_i-1, n_{i+1}+1, \ldots) \\ &- (W_a(n_{i-1}, n_i) + W_c(n_i, n_{i+1}))\, P(n_1,\ldots,n_L)\big]\theta(n_i). \end{aligned} \tag{6.7}$$

This align accounts for the net probability flux into and out of a given configuration due to single-particle hopping events. The gain terms correspond to particles arriving at site i from neighboring sites, while the loss terms account for particles leaving site i in either direction. The function $\theta(n_i)$ ensures that hopping events only occur from non-empty sites, enforcing local particle conservation. We shall be discussing the steady state behavior of this master align, that is,

$$\frac{d}{dt}P(n_1,\ldots,n_L;t) = 0. \tag{6.8}$$

However, the hopping rates given in equations 6.5 and 6.6 do not meet the criteria for a product measure in lattice systems with stochastic dynamics, where the rates are functions of both the departure and arrival sites, as outlined in [10].

6.4 Solution to the master equation when $U = 0$

The simplest possible case is when $U = 0$, then we have a ZRP like process with the effective hopping rates, provided there is a particle at the departure site is given as,

$$W_c = \frac{1+g}{2}, \quad W_a = \frac{1-g}{2}. \tag{6.9}$$

The master equation is then exactly solvable for any g, with all configurations equally likely, the measure of a given configuration is,

$$P(n_1, n_2, \ldots, n_L) = \frac{1}{\mathcal{Z}^0_{N,L}} \delta \left(\sum_{i=1}^{L} n_i - N \right), \tag{6.10}$$

where $\mathcal{Z}^0_{N,L}$ denotes the partition function for $U = 0$, given by,

$$\mathcal{Z}^0_{N,L} = \sum_{n_1=0}^{N} \cdots \sum_{n_L=0}^{N} \frac{1}{\binom{N+L-1}{L-1}} \delta \left(\sum_{i=1}^{L} n_i - N \right) \tag{6.11}$$

The formal expression of current $j(\rho, g)$ for $U = 0$ is given by,

$$j = \left\langle \frac{1+g}{2} \left(1 - \delta_{0,n_i}\right) - \frac{1-g}{2} \left(1 - \delta_{0,n_{i+1}}\right) \right\rangle \tag{6.12}$$

This reduces to,

$$j = g \left(1 - P(0)\right) \tag{6.13}$$

where, $P(0)$ is the probability that a site has no particles. We can write $P(0)$ as,

$$P(0) = \frac{1}{\mathcal{Z}^0_{N,L}} \sum_{n_2=0}^{N} \cdots \sum_{n_L=0}^{N} \frac{1}{\binom{N+L-1}{L-1}} \delta \left(\sum_{i=2}^{L} n_i - N \right) \tag{6.14}$$

$$= \frac{1}{\mathcal{Z}^0_{N,L}} \sum_{n_2=0}^{N} \cdots \sum_{n_L=0}^{N} \frac{L-1}{N+L-1} \frac{1}{\binom{N+L-2}{L-2}} \delta \left(\sum_{i=2}^{L} n_i - N \right)$$

$$P(0) = \frac{L-1}{N+L-1} \frac{\mathcal{Z}^0_{N,L-1}}{\mathcal{Z}^0_{N,L}} \tag{6.15}$$

In the thermodynamic limit of $L, N \to \infty$, but with a finite density we have,

$$P(0) = \frac{1}{1+\rho}. \tag{6.16}$$

This gives the thermodynamic expression for current by using 6.16 in 6.13,

$$j = g\frac{\rho}{1+\rho} \tag{6.17}$$

For small ρ, the current in $\mathcal{O}(\rho)$ is given by,

$$j \approx g\rho(1-\rho) \approx g\rho. \tag{6.18}$$

6.5 Solution to the Master Equation in the Limit $U \to \infty$: A Projection of States

The limit of infinite on-site interaction strength, $U \to \infty$, presents a particularly interesting regime. At first glance, the diverging interaction energy suggests a complete suppression of dynamics due to prohibitive energetic costs. However, a more careful analysis reveals an emergent effective dynamics within a reduced state space, characterized by the appearance of quasi-hardcore particles. This arises through a natural projection of the full configuration space Ω onto a constrained subspace $\omega \subset \Omega$.

In the steady state under strong interactions, the energetically favorable configuration corresponds to a uniform layering of particles across sites. Each site accommodates particles up to the nearest integer less than or equal to the global density, with the remaining particles distributed in a restricted manner. Specifically, we write the local occupation number at site i as

$$n_i = \rho_{\text{int}} + \tilde{m}_i, \tag{6.19}$$

where $\rho_{\text{int}} = \lfloor \rho \rfloor$ denotes the integer part of the density ρ, and $\tilde{m}_i \in \{0, 1\}$ represents an excess particle over this base filling. The binary variables $\tilde{m}_i$ encode the presence

(1) or absence (0) of these excess particles, which, as we show below, behave as emergent quasi-hardcore particles.

We consider the bias-free hopping rate between neighboring sites, defined as

$$W_c(n_i, n_{i+1}) = \exp\left[-\frac{\beta U}{2}(n_{i+1} - n_i + 1)\right](1 - \delta_{n_i,0}). \tag{6.20}$$

In the limit $U \to \infty$, the rate simplifies depending on the relative occupancies of the adjacent sites. The relevant asymptotic behaviors are as follows:

- Equal occupancies: If $n_i = n_{i+1}$, then

$$\lim_{U\to\infty} W_c(n_i, n_{i+1}) = \lim_{U\to\infty} \exp\left(-\frac{\beta U}{2}\right) \to 0. \tag{6.21}$$

- Empty departure site: If $n_i = 0$, then $W_c(n_i, n_{i+1}) = 0$ trivially due to the multiplicative factor.

- Departure site has one excess particle: If $n_i = n_{i+1} + 1$, i.e., there is an excess particle at the departure site, then

$$\lim_{U\to\infty} W_c(n_i, n_{i+1}) = \exp(0) = 1. \tag{6.22}$$

- Arrival site has one excess particle: If $n_i = n_{i+1} - 1$, then

$$\lim_{U\to\infty} W_c(n_i, n_{i+1}) = \exp\left(-\frac{\beta U}{2}\right) \to 0. \tag{6.23}$$

These asymptotic forms indicate that in the large-U limit, dynamics is effectively restricted to configurations where a single excess particle hops from a site to an adjacent site that lacks such an excess. This constraint leads to a simplified description in terms of the binary occupation numbers $\tilde{m}_i$, corresponding to quasi-hardcore particles that obey an exclusion principle (no two excess particles can occupy adjacent sites simultaneously).

The effective hopping rates for these quasi-hardcore particles can be expressed as:

$$W_c(\tilde{m}_i, \tilde{m}_{i+1}) = \frac{1+g}{2}\tilde{m}_i(1-\tilde{m}_{i+1}), \tag{6.24}$$

$$W_a(\tilde{m}_i, \tilde{m}_{i+1}) = \frac{1-g}{2}\tilde{m}_{i+1}(1-\tilde{m}_i),. \tag{6.25}$$

In summary, the $U \to \infty$ limit induces a projection of the dynamics onto a constrained subspace characterized by quasi-hardcore behavior, significantly simplifying the description of the system while retaining non-trivial collective dynamics.

Under these dynamics the probability of a given configuration which is effectively labeled by $\mathcal{C} = (\tilde{m}_1, \tilde{m}_2, \ldots, \tilde{m}_L)$ is given by,

$$P\left(\tilde{m}_1, \tilde{m}_2, \ldots, \tilde{m}_L\right) = \frac{1}{\binom{L}{M}}\delta\left(\sum_{i=1}^{L}\tilde{m}_i - M\right). \tag{6.26}$$

Here M is effective number of quasi particles, which is essentially,

$$\left(\sum_{i=1}^{L} n_i\right) - L\lfloor\rho\rfloor = M. \tag{6.27}$$

6.5.0.1 Periodic behavior of current

The formal expression for current will be given by,

$$j = \left\langle \frac{1+g}{2}\tilde{m}_i(1-\tilde{m}_{i+1}) - \frac{1-g}{2}\tilde{m}_{i+1}(1-\tilde{m}_i) \right\rangle \tag{6.28}$$

As seen in Chapter 3, in the thermodynamic limit, the steady state measure is a product measure and as result the current can be simplified to,

$$j = g\tilde{\rho}(1-\tilde{\rho}), \tag{6.29}$$

where we have,

$$\tilde{\rho} = \langle \tilde{m}_i \rangle \tag{6.30}$$

Since there is a uniform stacking of particle till the greatest integer function of ρ, the current is unit periodic in ρ. We make a final comment on the reduced state

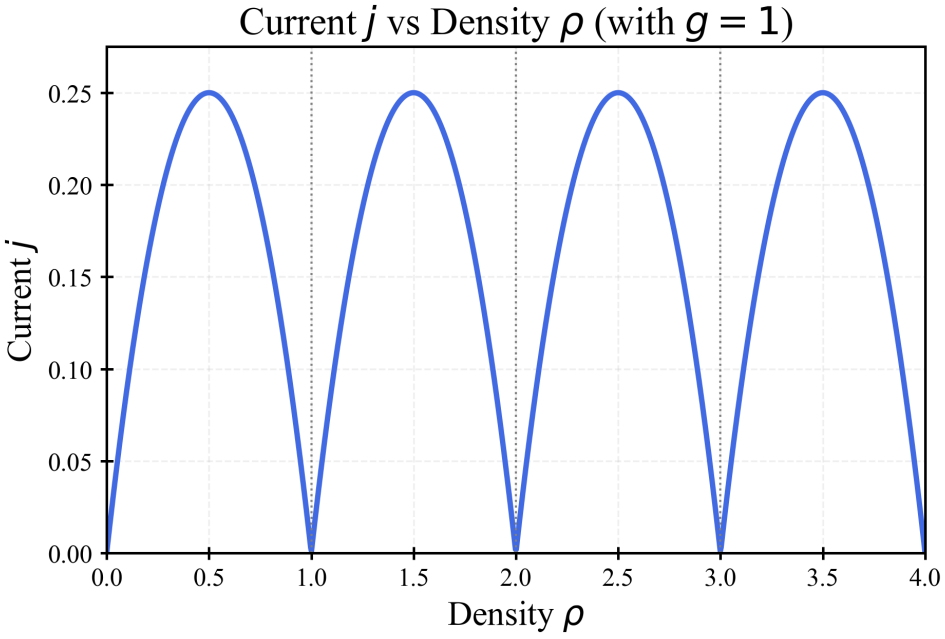

FIGURE 6.1: Plot of the current j as a function of density ρ for $g = 1$. The relation $j = g\,\tilde{\rho}(1-\tilde{\rho})$ governs the behavior, where $\tilde{\rho} = \rho - \lfloor\rho\rfloor$ is the fractional part of ρ. Peaks occur at half-integer values and drop to zero at integer densities, indicating periodicity in transport behavior.

space ω, which is a space of occupancies only of the form:

$$\omega \equiv \left\{ \{n_1, \ldots, n_L\} \text{ s.t. } \sum_{i=1}^{L} n_i = N \text{ and } n_i = \lfloor\rho\rfloor + \tilde{m}_i,\ \forall i \text{ and } \tilde{m}_i = \{0,1\}. \right\} \subset \Omega \tag{6.31}$$

where, Ω is a larger space with only one constraint,

$$\Omega \equiv \left\{ \{n_1, \ldots, n_L\} \text{ s.t. } \sum_{i=1}^{L} n_i = N \right\} \tag{6.32}$$

6.6 Solution to the Master Equation For $g = 0$.

Since we have developed the hopping rates from detailed balance at $g = 0$, the steady state weight for $g = 0$ is particularly simple, namely the weight of a given

configuration is given by the Boltzmann weights,

$$P(n_1, n_2, \ldots, n_L) = \frac{1}{\mathcal{Z}_{N,L}} \prod_{i=1}^{L} exp\left(-\frac{\beta U}{2} n_i(n_i - 1)\right) \delta\left(\sum_{i=1}^{L} n_i - N\right), \tag{6.33}$$

where, the canonical partition function is given as,

$$\mathcal{Z}_{N,L} = \sum_{n_1=0}^{N} \cdots \sum_{n_L=0}^{N} exp\left(-\frac{\beta U}{2} n_i(n_i - 1)\right) \delta\left(\sum_{i=1}^{L} n_i - N\right). \tag{6.34}$$

Since the system is translationally invariant we have,

$$\rho = \frac{N}{L}. \tag{6.35}$$

In the grand canonical ensemble, all sites are decoupled to each other and the single site grand partition function is given by,

$$\mathcal{Z}_1 = \sum_{n=0}^{\infty} z^n exp\left(-\frac{\beta U}{2} n(n-1)\right) \tag{6.36}$$

To approximate this sum, we apply the Euler-Maclaurin formula [9] truncated to include only the integral and boundary correction term:

$$\mathcal{Z}_1 \approx \frac{1}{2} + \frac{1}{2}\sqrt{\frac{2\pi}{\beta U}} \exp\left(\frac{\left(\ln z + \frac{\beta U}{2}\right)^2}{2\beta U}\right) \left[1 + \operatorname{erf}\left(\frac{\ln z + \frac{\beta U}{2}}{\sqrt{2\beta U}}\right)\right]. \tag{6.37}$$

To validate the Euler-Maclaurin approximation, we compare it with the original sum in Fig. 6.2. The close agreement across the fugacity range confirms the reliability of the approximation under the chosen parameters.

6.7 Numerical Results

For intermediate values of βU and g, we could not find an analytic form of the steady state solution, and hence we employed standard Monte Carlo (MC) simulation techniques. Below, we outline the procedure in the context of periodic boundary conditions:

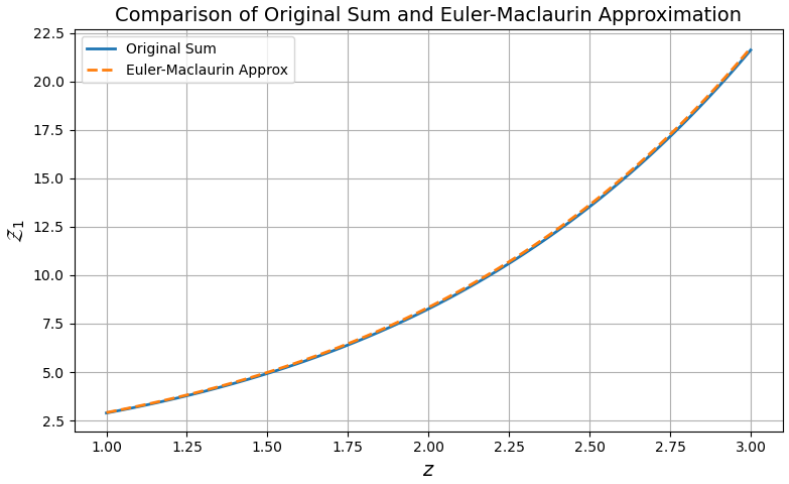

FIGURE 6.2: Comparison between the original partition function sum $\mathcal{Z}_1(z)$ and its Euler-Maclaurin approximation. The figure demonstrates excellent agreement between the two expressions across a range of fugacity values z. Parameters used: $\beta = 1.0$, $U = 0.5$, and $n_{\max} = 500$. n_{max} denotes the maximum number of terms taken while numerically calculating the sum.

- We initialize the system on a one-dimensional lattice of length L, assigning arbitrary occupancies n_i to each site i. The total particle density is fixed and defined as,

$$\rho = \frac{1}{L}\sum_{i=1}^{L} n_i.$$

- At each micro-step, a site i is selected uniformly at random. If the selected site is unoccupied ($n_i = 0$), the micro-step count is incremented by one, and no further action is taken.

- If the site is occupied, a direction is chosen probabilistically: clockwise with probability $\frac{1+g}{2}$ and anti-clockwise with probability $\frac{1-g}{2}$. This selection defines a bond between the departure site i and the arrival site j (either $i+1$ or $i-1$ modulo L due to periodic boundaries), with respective occupancies (n_i, n_j).

- A particle is proposed to hop from site i to site j, updating the configuration as $(n_i, n_j) \to (n_i - 1, n_j + 1)$. This move is accepted with probability

$$p = \min\left\{1, e^{-\beta\Delta E}\right\}, \tag{6.38}$$

where the energy change ΔE associated with the move is given by

$$\Delta E = U(n_j - n_i + 1). \tag{6.39}$$

- One full Monte Carlo step (MCS) consists of L such micro-steps. We thermalize the system by performing $10L^2$ MCS before beginning any measurements. Observables such as correlation functions and particle current are then recorded every 10 MCS to mitigate autocorrelation effects.

This algorithm successfully replicated the limiting cases of the coupling constant, and biasing parameter and in the regimes where the measure is known besides giving insight in the intermediate regimes of g and βU.

6.7.1 Connected Correlation function

We define the two point density-density correlation function as,

$$G(r) = \langle n_i n_{i+r} \rangle - \langle n_i \rangle \langle n_{i+r} \rangle. \tag{6.40}$$

From the translational invariance of the system, and due to repulsive interactions there is no condensation in the system we have for any i,

$$\langle n_i \rangle = \frac{N}{L} = \rho. \tag{6.41}$$

Thus, we have,

$$G(r) = \langle n_i n_{i+r} \rangle - \rho^2. \tag{6.42}$$

We numerically obtained the variance at each site, $G(0)$ and the nearest neighbor correlation function $G(1)$. For larger values of r, the correlation function is negligibly small.

As shown in Figure 6.3, the site-wise variance decreases with increasing U, since larger values of U constrain the system to a subspace of configurations. Consequently, the variance approaches the expected hardcore limit, indicated in the figure. The nearest-neighbor correlation function $G(1)$ exhibits non-monotonic behavior with respect to βU: it vanishes in both the ZRP and ASEP limits, leading to

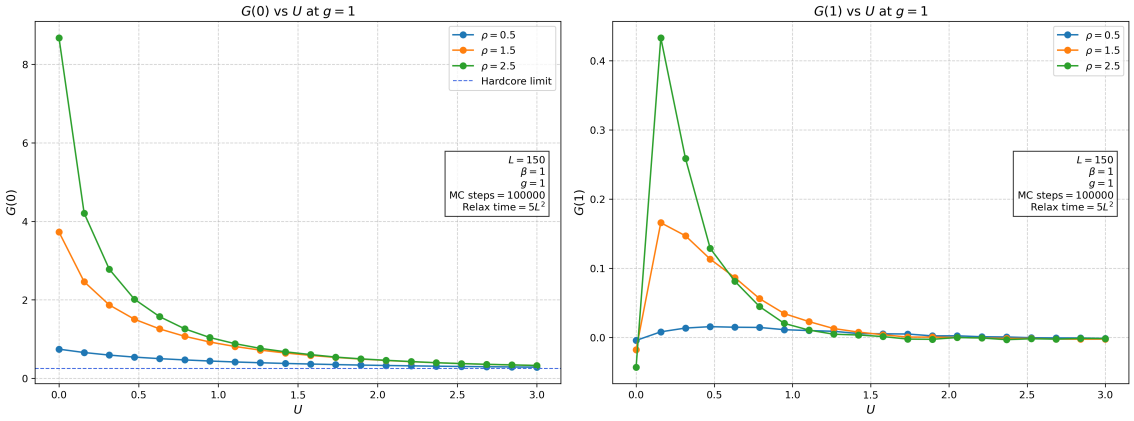

FIGURE 6.3: Comparison of $G(0)$ and $G(1)$ as functions of U for different densities ρ at $g = 1$.

a peak at some intermediate U, after which it declines. The small negative value observed at $U = 0$ is a finite-size effect. The emergence of correlations reflects the breakdown of the product measure, as discussed in [10].

Additionally, our numerical results indicate that correlations become more pronounced as $g \to 1$. This is intuitively reasonable—when $g = 0$, the system is in equilibrium, while increasing asymmetry introduces dynamic constraints that induce correlations between neighboring sites, due to the dependence of hopping rates on both the departure and arrival sites. In contrast, the variance is only weakly affected by g. This behavior is illustrated in Figure 6.4.

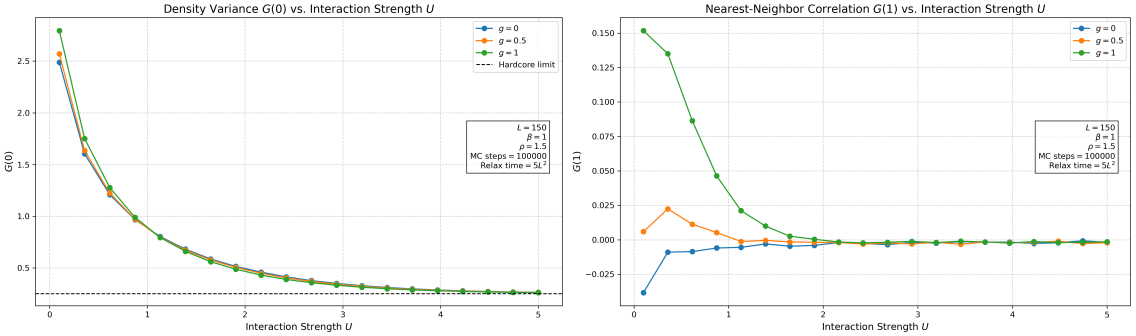

FIGURE 6.4: Comparison of $G(0)$ and $G(1)$ as functions of U for different densities ρ at $g = 1$.

6.7.2 Current

We have also numerically studied the current formally defined using the expressions in 6.5 and 6.6,

$$j = \langle W_c - W_a \rangle \,, \tag{6.43}$$

The current when plotted against g for relatively low values of βU has a linear relation in g and keeps decreasing for larger βU while being bounded from below by the hardcore limit as seen in Figure 6.5 We also plot the current j as a function

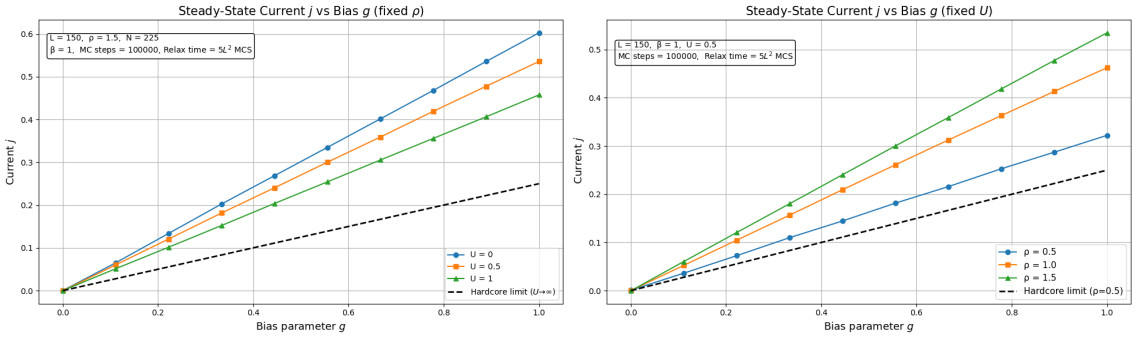

FIGURE 6.5: Comparison of current j as functions of g for different densities ρ and different U

of the density ρ for various interaction strengths. A saturation in the current is observed at higher densities due to repulsive interactions. In contrast, for $U = 0$, the current increases without bound. At large values of βU, oscillatory behavior emerges, consistent with predictions in the strong interaction limit. When the interaction strength is held fixed, the current magnitude increases with g, eventually saturating at high densities due to the repulsive nature of the interactions. These results are illustrated in Figure 6.7.

We also plotted the current j as a function of the interaction strength U, and again observed saturation of the current at the effective fractional density in the large βU limit. Notably, the currents for densities $\rho = 0.5$ and $\rho = 1.5$ converge to the same value, while the current for $\rho = 1$ vanishes as U becomes large. As expected, increasing g leads to a higher current, which eventually saturates at large U.

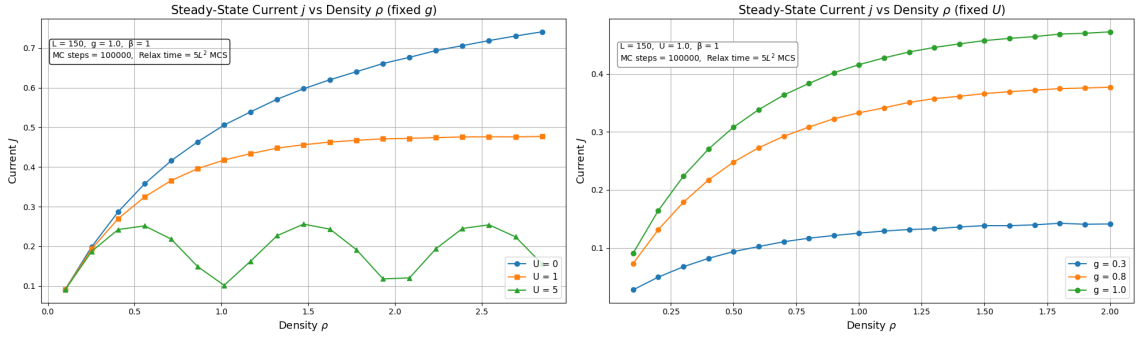

FIGURE 6.6: Comparison of current j as functions of ρ for different biasing strength g and different U

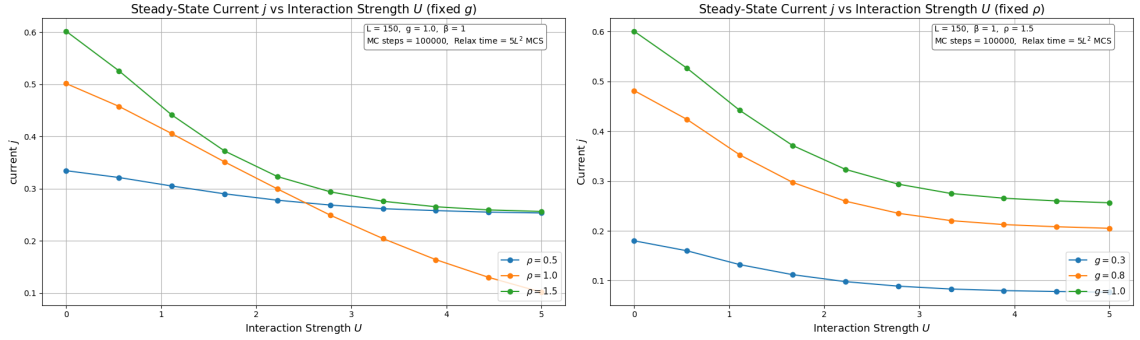

FIGURE 6.7: Comparison of current j as functions of ρ for different biasing strength g and different U

6.7.3 Order Parameter

A way to characterize the behavior of an ASEP like limit, can be realized through an order parameter ϕ, which is defined as,

$$\phi = \langle \max \{n_i\}_{\forall i} \rangle \tag{6.44}$$

In the limit, $\beta U \to \infty$, for a given density ρ, ϕ converges to the greatest integer function of ρ.

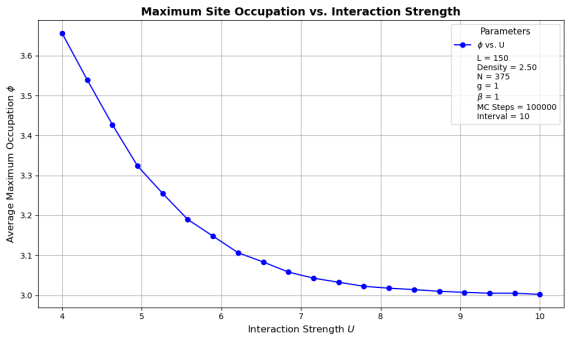

FIGURE 6.8: Order Parameter ϕ v/s U for fixed ρ, g.

6.8 Phase diagram

Our discussion of the limiting cases and the numerical results can be summarized in the form of a phase diagram shown in Figure 6.9.

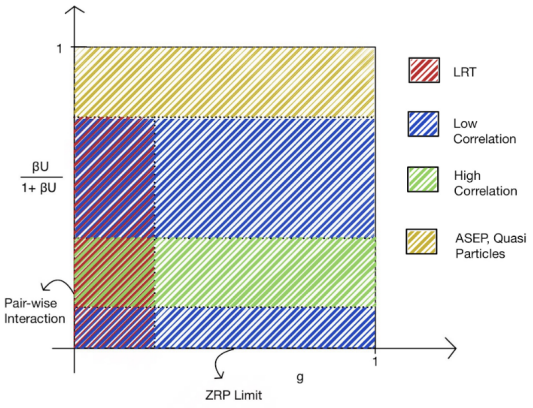

FIGURE 6.9: Phase Diagram

6.9 Numerical Results in Open Boundary Conditions

We have also investigated the same dynamics, previously defined under periodic boundary conditions, in the case of reflecting boundary conditions. A step-like structure in the density profile ρ is again observed when

$$\frac{1+g}{1-g} < e^{\beta U}. \tag{6.45}$$

The Monte Carlo simulation method used is the same as described in the previous section. As shown in Figure 6.10, these step features become more pronounced for larger values of g, resulting from the interplay between the external bias g and the interaction strength βU. In the bias-dominated regime, as illustrated in Figure 6.11,

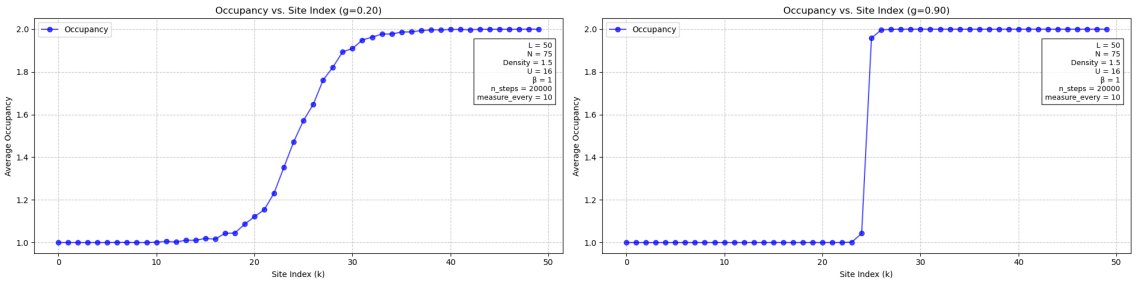

FIGURE 6.10: Comparison of density ρ_k as a function of k for a large βU and g

the density exhibits a linear increase beyond a certain site index k_0, as shown in the plots below. For site indices less than k_0, a region emerges where all sites remain completely empty. This behavior arises because the strong rightward bias drives particles toward the end of the system. However, due to the presence of repulsive interactions, the particles are unable to accumulate entirely at the final site, leading instead to a spread in density beyond k_0.

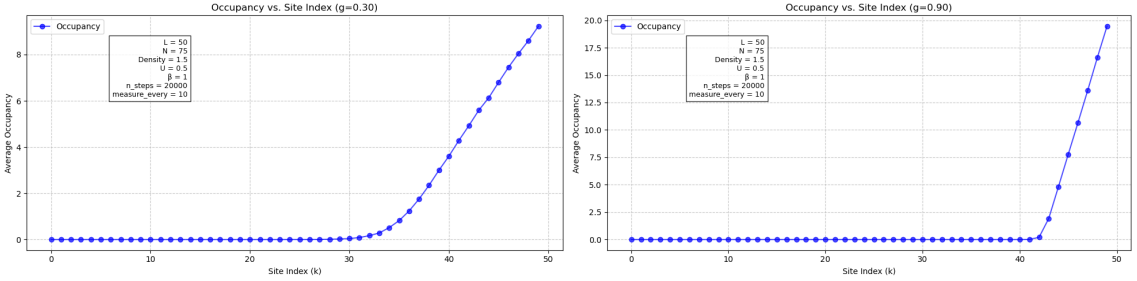

FIGURE 6.11: Comparison of density ρ_k as a function of k for a given g and small βU.

This concludes our discussion on this chapter, a more detailed analysis of the reflecting boundary condition is left as a future study.

This page is intentionally left blank.

Chapter 7

Conclusion

7.1 Conclusion

In this study, we examined a class of non-equilibrium systems under simple geometries, such as periodic and reflecting boundary conditions, as well as disordered structures like random combs. We observed several features, including limiting behaviors, correlated regimes, ASEP like limits, and step-like patterns in density profiles. These findings were supported through both numerical simulations and analytical arguments.

There are several directions in which this work could be extended. Some possible future steps include:

- Developing analytical methods to solve the master equation 6.7 under periodic boundary conditions. This could involve:
  - Applying perturbation theory to the transition rate matrix $\mathbb{W}$ and solving the steady state in terms of βU and g.
  - Mapping the dynamics to a path integral formulation and analyzing it using standard perturbative techniques.
- Studying the system's relaxation to the steady state and exploring whether a hydrodynamic description can be formulated.

- Investigating the different limiting cases in quantum settings, especially in light of similarities with the Bose–Hubbard model.

These directions may help in building a more complete understanding of the system's behavior beyond the scope of this work.

This page is intentionally left blank.

Bibliography

[1] R. K. Pathria and P. D. Beale, *Statistical Mechanics*. Elsevier, 3rd ed., 2011.

[2] B. Derrida, "An exactly solvable non-equilibrium system: the asymmetric simple exclusion process," *Physics Reports*, vol. 301, no. 1-3, pp. 65–83, 1998.

[3] N. G. Van Kampen, *Stochastic Processes in Physics and Chemistry*. Elsevier, 3rd ed., 2007.

[4] M. R. Evans and T. Hanney, "Nonequilibrium statistical mechanics of the zero-range process and related models," *Journal of Physics A: Mathematical and General*, vol. 38, no. 19, pp. R195–R240, 2005.

[5] B. Derrida, M. Evans, V. Hakim, and V. Pasquier, "Exact solution of a 1d asymmetric exclusion model using a matrix formulation," *Journal of Physics A: Mathematical and General*, vol. 26, no. 7, pp. 1493–1517, 1993.

[6] M. Barma and D. Dhar, "Directed diffusion in a percolation network," *Journal of Physics C: Solid State Physics*, vol. 16, no. 8, pp. 1451–1458, 1983.

[7] R. Ramaswamy and M. Barma, "Transport in random networks in a field: interacting particles," *Journal of Physics A: Mathematical and General*, vol. 20, no. 10, pp. 2973–2985, 1987.

[8] E. Duchon, Y. L. Loh, and N. Trivedi, "Optical lattice emulators: Bose and fermi hubbard models," *arXiv:1311.0543v1*, 2013.

[9] T. M. Apostol, "An elementary view of euler's summation formula," *The American Mathematical Monthly*, vol. 106, no. 5, pp. 409–418, 1999.

[10] M. R. Evans and B. Waclaw, "Condensation in stochastic mass transport models: beyond the zero-range process," *arXiv preprint arXiv:1312.5642*, 2013.